journal

J. Am. Ceram. Soc., 84 [2] 353–58 (2001)

Thermal Conductivity of β-Si_3N_4: III, Effect of Rare-Earth (RE = La, Nd, Gd, Y, Yb, and Sc) Oxide Additives

Mikito Kitayama*,†

Synergy Ceramics Laboratory, Fine Ceramics Research Association, 2268-1 Simo-Shidami, Moriyama-ku, Nagoya, Aichi 463-8687 Japan

Kiyoshi Hirao,* Koji Watari,* Motohiro Toriyama, and Shuzo Kanzaki*

National Industrial Research Institute of Nagoya, 2268-1 Simo-Shidami, Moriyama-ku, Nagoya, Aichi 463-8687 Japan

β-Si_3N_4 ceramics sintered with a series of rare-earth (RE = La, Nd, Gd, Y, Yb and Sc) oxide additives were fabricated by hot pressing and subsequent annealing. Their microstructures, lattice oxygen contents, and thermal conductivities were evaluated. Mean grain size increased, while lattice oxygen content decreased, and hence, thermal conductivity increased with decreasing ionic radius of the rare-earth element. In all cases, a marked change was observed in the order of ionic radius from La to Nd to Gd, and a little change was observed below them. Rare-earth oxide additives significantly influenced the thermal conductivity of β-Si_3N_4, unlike in the case of AlN.

I. Introduction

One of our previous works (Part I)[1] investigated the effects of various microstructural factors (grain size, thickness of the grain boundary film, and alignment of elongated grains) of β-Si_3N_4 ceramics on thermal conductivity. Theoretically and experimentally, it was demonstrated that mere grain growth could not improve thermal conductivity, because of the unique faceting nature of this material. Another work (Part II)[2] reported that the lattice oxygen content controlled the thermal conductivity of β-Si_3N_4 ceramics just as in the case of AlN ceramics. The relationship between the microstructure, grain-boundary phase, lattice oxygen content, and thermal conductivity of β-Si_3N_4 that was sintered at various Y_2O_3/SiO_2 additive ratios was clarified. It was suggested that there was an optimum amount of sintering additive depending on the amount of oxygen impurity in the Si_3N_4 raw powder. Although grain growth improves thermal conductivity at the expense of strength, decreasing the lattice oxygen content with less grain growth has an advantage with this material—high strength. Because sintering additives play key roles in densification, phase transformation, microstructural control, and oxygen removal of Si_3N_4 ceramics, a search for the most suitable sintering additive is crucial for this purpose.

Rare-earth oxides (RE_2O_3) have been widely investigated as sintering additives for Si_3N_4.[3–12] Rare-earth elements including Sc, Y, and lanthanides (Ln) have a common ionic valence z of +3, and are known to be the most electropositive elements. Thus, it has been suggested that they are suitable sintering additives for Si_3N_4.[13,14] Because lanthanide elements continuously decrease their ionic radii r with increasing atomic number, known as lanthanide contraction, their cationic field strengths z/r^2 also continuously change with their atomic number. This causes substantial variations in the various properties of Ln-Si-(Al)-O-N glasses[15–18] that are the grain boundary phase of Si_3N_4 ceramics sintered with rare-earth oxide additives, and thus, can also affect various properties of Si_3N_4 ceramics themselves. It has been observed that the mean aspect ratio at the end of the phase transformation is proportional to the ionic radius of rare-earth elements.[19] Recently, we observed that rare-earth elements have an influence not only during phase transformation but also during Ostwald ripening.[20] This work clearly showed that rare-earth oxide additives significantly affect the grain growth behavior of Si_3N_4 during and after phase transformation, which influences the purification kinetics of the β-Si_3N_4 crystal lattice that proceed via a solution–reprecipitation mechanism through the liquid phase. Furthermore, the variation of the grain boundary phase due to different rare-earth oxide additives can change the thermodynamics, and hence the lattice oxygen content of β-Si_3N_4. Although a series of rare-earth oxide additives did not show any significant difference or trend for the thermal conductivity of AlN,[21] it might do so for β-Si_3N_4 for the reasons mentioned above. The purpose of this work is to investigate the effect of various rare-earth oxide additives on the thermal conductivity of β-Si_3N_4 ceramics from two points of view, microstructure and lattice oxygen.

II. Experimental Procedure

Commercial α-Si_3N_4 powder (SN-E05, specific surface area 4–6 m^2/g, oxygen content 0.84 wt%; UBE Industries, Ltd., Japan) was mixed with RE_2O_3 powders (RE = La, Nd, Gd, Y, Yb, and Sc; purity >99.9%, specific surface areas = 3–5 m^2/g; Nihon Yttrium Co. Ltd., Tokyo, Japan) in a resin-coated ball-mill for 3 h using methanol as a mixing medium. The molar ratios of the mixtures were fixed at Si_3N_4:RE_2O_3 = 20:1. Each slurry was dried using a rotary evaporator at 60°C, subsequently dried at 110°C for 2 h, and passed through a 60-mesh nylon sieve; 30 g of each mixed powder was charged into a 30 mm ϕ high-purity graphite dye (Toyotanso Co., Japan) coated with high-purity boron nitride powder (GP grade, Denki Kagaku Kogyo Co., Japan), and hot-pressed at 1800°C for 2 h under a pressure of 40 MPa in a flowing nitrogen atmosphere. These conditions resulted in sintered bodies with more than 99% of theoretical density. The hot-pressed sintered bodies were subsequently annealed at 1850°C for 4 and 16 h under a nitrogen pressure of 1 MPa in a high-purity BN crucible (N1 grade, Denki Kagaku Kogyo Co., Japan) with a powder bed consisting of a mixture of Si_3N_4 (UBE SN-E10 grade):BN (GP grade) = 7:3. It should be noted that hot pressing and annealing were conducted in a furnace with graphite heating

R. A. Cutler—contributing editor

Manuscript No. 188781. Received January 25, 2000; approved September 20, 2000.

This work has been supported by the Agency of Industrial Science and Technology, Ministry of International Trade and Industry, Japan, as part of the Synergy Ceramics Project. Part of the work has been supported by the New Energy and Industrial Technology Development Organization. The authors are members of the Joint Research Consortium of Synergy Ceramics.

*Member, American Ceramic Society.

†Current address: Fukuoka Institute of Technology, 3-30-1 Wajiro-higashi, Higashi-ku, Fukuoka, 811-0295, Japan.

elements that had never been used for materials containing aluminum. By combining this with the use of a resin-coated ball-mill and a high-purity graphite dye, extreme care was taken to avoid any possible contamination. Phase identification of the sintered bodies was performed by X-ray diffraction (XRD). Specimen densities were determined by the Archimedes method.

Disk specimens for measuring thermal diffusivity (10 mm $\phi \times$ 2 mm thick) were prepared parallel and perpendicular to the hot-pressed surfaces from all of the sintered samples as illustrated in Fig. 1. These are called the "para" and "perp" specimens, respectively. The samples were finished using a 75 μm diamond wheel. Thermal diffusivity was measured by the laser-flash method (TC-3000, ULVAC, Japan) after coating both sides of the specimens with a 600 Å thick layer of gold and subsequently with a black carbon layer. Thermal conductivity k was calculated according to the equation

$$k = \rho \cdot C_p \cdot \alpha \quad (1)$$

where ρ, C_p, and α are the density, the specific heat, and the thermal diffusivity, respectively. A constant value of specific heat, 0.7 J/(g·K), was used in this work, because it was reported that the specific heat of dense β-Si_3N_4 ceramics was almost constant.[22] After the thermal diffusivities were measureed, all disk specimens were polished using a 1 μm diamond slurry, plasma-etched in CF_4 gas, coated with a 200 Å thick layer of gold, and observed by the scanning electron microscope (SEM) (JSM-6340F, JEOL, Japan). Mean grain sizes were determined from SEM photographs using the linear intercept method.

The lattice oxygen content of the dense sintered Si_3N_4 body was analyzed using a method developed in the previous paper.[2] A 1 g sample of each sintered body was ground in a WC ball-mill for 10 min, dispersed in 50 mL of methanol, passed through a 500 mesh (25 μm) sieve, and dried at 60°C. Each powder was treated with 50% HF at 60°C for 3 h, and then 50% H_2SO_4 at 120°C for 2 h to remove the grain boundary phase and possible fluoride compounds, respectively. After being washed three times with distilled water, each powder was dried at 110°C for 12 h, and passed through a 100 mesh (150 μm) nylon sieve. A commercial hot gas extraction analyzer (TC-436, LECO Co., St Joseph, MI) was used for oxygen and nitrogen determinations. About 20 mg of each dried powder sample was weighed into a graphite crucible (10 mm $\phi \times$ 16 mm), and about 200 mg of graphite powder (No. 501-073, LECO Co., St Joseph, MI) was added to the sample to accelerate the carbothermal reduction of the oxide phases. A crucible was heated up to 2500°C in 5 min in a flowing Ar atmosphere. The release of oxygen and nitrogen as a function of temperature, and total concentrations of oxygen and nitrogen, were recorded. A total of three measurements were performed for all samples.

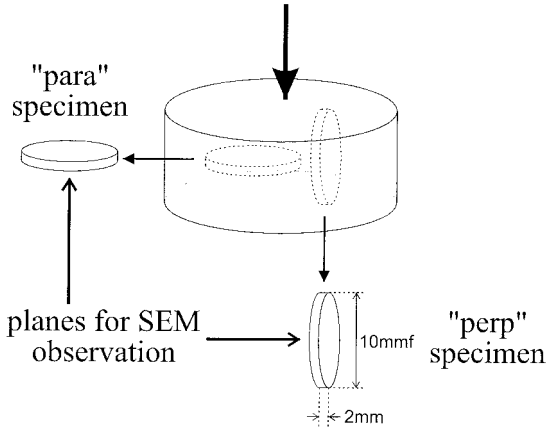

Fig. 1. Illustration showing how the disk specimens (10 mm $\phi \times$ 2 mm) were taken from the sintered samples.

III. Results

(1) Grain Boundary Phase Identification

The RE_2O_3/SiO_2 molar ratio considering oxygen content of the raw α-Si_3N_4 powder is about 1.36. According to the results obtained in the previous paper,[2] this ratio gives the grain boundary phases of $Y_{20}N_4Si_{12}O_{48}$ (N-apatite) and $Y_2Si_3O_3N_4$ (melilite) and the lowest lattice oxygen content when Y_2O_3 was used as a sintering additive. It was concluded that the grain boundary phase dictated the thermal conductivity of β-Si_3N_4. Thus, it is particularly important to know what kinds of phases are formed for different rare-earth oxide additives. Table I summarizes the results of XRD phase identification of samples annealed for 4 and 16 h. Only a sample sintered with La_2O_3 at 1850°C for 4 h contained a significant amount of the α-phase (about 44%). None of the other samples contained the α-phase. All of the rare-earth oxide additives showed a large and broad peak that is characteristic of the amorphous grain boundary phase. In addition to it, a variety of crystalline phases were observed for different rare-earth oxide additives even though the same molar ratio was used for all additives. For Sc_2O_3, only Sc_2SiO_5 (RE_2O_3:SiO_2 = 1:1) was identified. For La_2O_3, both $La_{20}N_4Si_{12}O_{48}$ (RE_2O_3:SiO_2 = 10:9) and La_2SiO_5 (RE_2O_3:SiO_2 = 1:1) were identified. For Nd_2O_3, both $Nd_2Si_3O_3N_4$ (RE_2O_3:SiO_2 = 1:0) and $Nd_4Si_3O_{12}$ (RE_2O_3:SiO_2 = 2:3) were identified. For Y_2O_3 and Gd_2O_3, both $RE_{20}N_4Si_{12}O_{48}$ (RE_2O_3:SiO_2 = 10:9) and $RE_2Si_3O_3N_4$ (RE_2O_3:SiO_2 = 1:0) were identified. For Yb_2O_3, only $Yb_4Si_2N_2O_7$ (RE_2O_3:SiO_2 = 4:1) was identified. Considering the RE_2O_3/SiO_2 molar ratio of the powder compact, all of these phases are confirmed to be possible referring to the phase diagrams of Si_3N_4–SiO_2–RE_2O_3 systems.[23]

(2) Microstructure and Thermal Conductivity

Figure 2 shows SEM photographs of polished and etched surfaces of samples annealed for 16 h. All photographs are for the "para" specimens so that elongated β-grains tend to lie along the plane of the SEM observation. Evidently, grain size markedly increases in the inverse order of the ionic radius of rare-earth oxides from La to Nd to Gd, and a little change was observed below them.

Table II summarizes ionic radii of rare-earth atoms, densities, grain sizes, thermal diffusivities, and thermal conductivities of the "para" and "perp" specimens for all sintered samples. From Fig. 1, it is easy to understand that measured thermal conductivities are the values perpendicular to the planes observed by SEM, and hence, mean grain sizes of the "para" and "perp" specimens correspond to the thermal conductivities of the "perp" and "para" specimens, respectively. The differences in mean grain size between the "para" and "perp" specimens are quite small, probably because of the method for determining grain sizes. What the linear intercept method determines is very close to grain width due to the rodlike grain shape of β-Si_3N_4. Thermal conductivities of the "para" specimens are always smaller than those of the "perp" specimens. This is because of the alignment of elongated β-grains due to the hot-pressing as pointed out in the previous paper.[1]

From Table II, it is evident that the grain growth behavior and thermal conductivity of β-Si_3N_4 ceramics closely relate to the ionic radii of rare-earth atoms. Figure 3 shows the relationship between the ionic radii of rare-earth additives and mean grain sizes of the "para" and "perp" specimens. Mean grain size steeply increases with decreasing ionic radius in the order La, Nd, and Gd, and reaches almost a constant value. Figure 4 shows the relationship between the ionic radii of rare-earth elements and thermal conductivities of β-Si_3N_4 sintered bodies. It reveals the same trend as mean grain size. According to Eq. (1), thermal conductivity is a function of density, and thus, a heavier rare-earth atom should give a higher thermal conductivity value. To eliminate the effect of density, the relationship between ionic radii of rare-earth atoms and thermal diffusivities of β-Si_3N_4 sintered bodies is plotted in Fig. 5. It is observed that thermal diffusivity consistently decreases with increasing ionic radius.

Table I. XRD Phase Identification Result

Additive	Annealing time (h)	Phase (intensity)[†]
La_2O_3	4	β-Si_3N_4 (s), α-Si_3N_4 (s), $La_{20}N_4Si_{12}O_{48}$ (m), La_2SiO_5 (w)
	16	β-Si_3N_4 (vs), $La_{20}N_4Si_{12}O_{48}$ (m), La_2SiO_5 (w)
Nd_2O_3	4	β-Si_3N_4 (vs), $Nd_2Si_3O_3N_4$ (w), $Nd_4Si_3O_{12}$ (w)
	16	β-Si_3N_4 (vs), $Nd_2Si_3O_3N_4$ (w), $Nd_4Si_3O_{12}$ (w)
Gd_2O_3	4	β-Si_3N_4 (vs), $Gd_{20}N_4Si_{12}O_{48}$ (m), $Gd_2Si_3O_3N_4$ (vw)
	16	β-Si_3N_4 (vs), $Gd_{20}N_4Si_{12}O_{48}$ (m), $Gd_2Si_3O_3N_4$ (w)
Y_2O_3	4	β-Si_3N_4 (vs), $Y_{20}N_4Si_{12}O_{48}$ (m), $Y_2Si_3O_3N_4$ (w)
	16	β-Si_3N_4 (vs), $Y_{20}N_4Si_{12}O_{48}$ (m), $Y_2Si_3O_3N_4$ (w)
Yb_2O_3	4	β-Si_3N_4 (vs), $Yb_4Si_2N_2O_7$ (s)
	16	β-Si_3N_4 (vs), $Yb_4Si_2N_2O_7$ (s)
Sc_2O_3	4	β-Si_3N_4 (vs), Sc_2SiO_5 (vw)
	16	β-Si_3N_4 (vs), Sc_2SiO_5 (vw)

[†]vs = very strong, s = strong, m = middle, w = weak, vw = very weak.

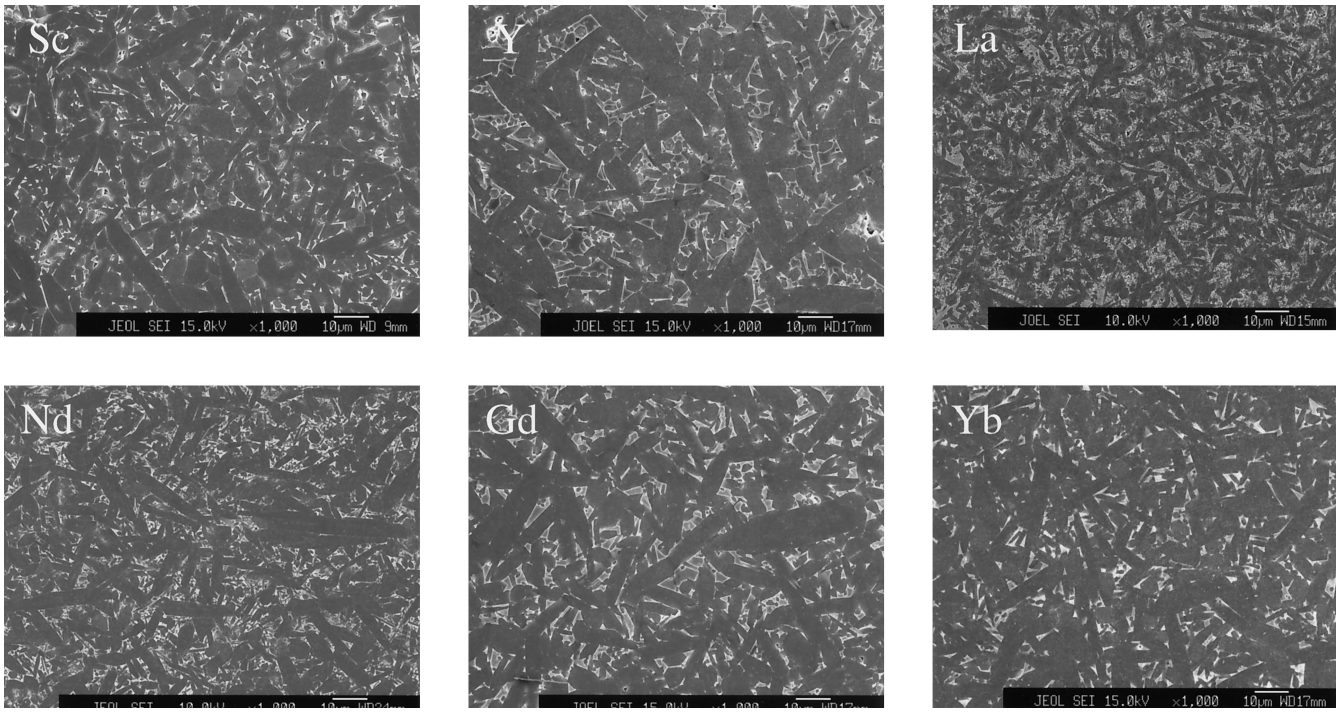

Fig. 2. SEM photographs of the "para" specimens of β-Si_3N_4 sintered with rare-earth (Sc, Y, La, Nd, Gd, and Yb) oxide additives.

Since both mean grain sizes and thermal diffusivities of β-Si_3N_4 sintered with various rare-earth oxide additives possess approximately the same trend against ionic radii, a correlation between them is expected. Figure 6 compares the grain size–thermal diffusivity relationship obtained in this work with the previous data for 5 wt% Y_2O_3 hot-pressed Si_3N_4.[1] It is observed that all of the data points scatter along the lines of the previous data.

(3) Lattice Oxygen Content

Table II also shows the lattice oxygen contents of β-Si_3N_4 sintered with different rare-earth oxide additives determined by the hot gas extraction method. Figure 7 shows the relationship between ionic radii of rare-earth oxide additives and lattice oxygen contents of β-Si_3N_4. Since a sample sintered with La_2O_3 at 1850°C for 4 h contains a significant amount of the α-phase that contains about 0.83 wt% oxygen, its data are excluded from this figure. It is found that the oxygen content in the β-Si_3N_4 crystal lattice decreases with decreasing ionic radius from La to Nd to Gd, and reaches almost a constant value below them. Figure 8 shows the relationship between the lattice oxygen content and thermal diffusivity of β-Si_3N_4 sintered with various rare-earth oxide additives, demonstrating a good inverse correlation. The lattice oxygen content decreases with increasing annealing time except in the case of Yb. The reason for this exception will be discussed below.

IV. Discussion

(1) Effect of Microstructure on Thermal Conductivity

As reported in Part I,[1] grain size significantly influences the thermal conductivity of β-Si_3N_4 ceramics through the effect that it changes the number of grain boundary films per unit length. Thus, the larger the mean grain size, the higher the thermal conductivity. Hence, at this stage, we can explain the difference in thermal conductivity simply by the difference in the mean grain size of β-Si_3N_4 sintered with various rare-earth oxide additives.

It is well known that the phase transformation and Ostwald ripening of Si_3N_4 proceed via solution–reprecipitation in the liquid phase that is formed at high temperature by the reaction between sintering additives, Si_3N_4, and SiO_2 derived from the oxygen impurity of the raw powder. The kinetics of these processes are indeed affected by the viscosity and wetting behavior of the liquid phase. However, as reported elsewhere,[20] the interfacial reaction rate between the prismatic facet of the β-Si_3N_4 crystal and the liquid phase is the most influential in this material. It was found that grain growth of β-Si_3N_4 shifts from interfacial-reaction-

Table II. Ionic Radii of Rare-Earth Elements, Densities, Grain Sizes, Thermal Diffusivities, and Thermal Conductivities of the "para" and "perp" Specimens, and Lattice Oxygen Contents for All Sintered Samples

Additive	Ionic radius (Å)	Annealing time (h)	Density (g/cm^3)	Grain size (μm)		Thermal diffusivity (m^2/s)		Thermal conductivity (W/(m·K))		Lattice oxygen (%)
				para	perp	para	perp	para	perp	
La_2O_3	1.06	4	3.351	N/A	N/A	0.1200	0.1349	28.1	31.6	0.2794 ± 0.0371
		16	3.327	1.38	1.27	0.2195	0.2787	51.1	64.9	0.1163 ± 0.0055
Nd_2O_3	1.00	4	3.396	1.24	0.85	0.2698	0.3434	64.1	81.6	0.0942 ± 0.0045
		16	3.379	2.39	2.06	0.3054	0.4141	72.2	97.9	0.0923 ± 0.0134
Gd_2O_3	0.94	4	3.421	4.14	3.78	0.3288	0.4204	78.7	100.7	0.0765 ± 0.0024
		16	3.420	4.74	4.00	0.3408	0.4465	81.6	106.9	0.0692 ± 0.0126
Y_2O_3	0.89	4	3.252	4.58	4.16	0.3641	0.4597	82.9	104.6	0.0765 ± 0.0013
		16	3.277	4.79	4.25	0.3607	0.4612	82.7	105.8	0.0632 ± 0.0018
Yb_2O_3	0.86	4	3.462	3.85	3.73	0.3554	0.4744	86.1	115.0	0.0615 ± 0.0022
		16	3.442	3.94	3.64	0.3678	0.4759	88.6	114.7	0.0802 ± 0.0065
Sc_2O_3	0.73	4	3.231	3.61	3.46	0.3754	0.4457	84.9	100.8	0.0851 ± 0.0038
		16	3.198	4.57	4.44	0.4001	0.4749	89.6	106.3	0.0775 ± 0.0035

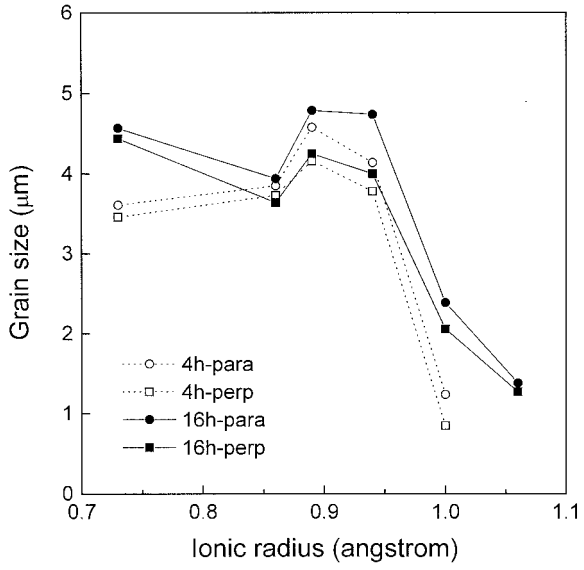

Fig. 3. Relationship between the ionic radii of rare-earth additives and mean grain sizes of the "para" and "perp" specimens of β-Si_3N_4 sintered bodies.

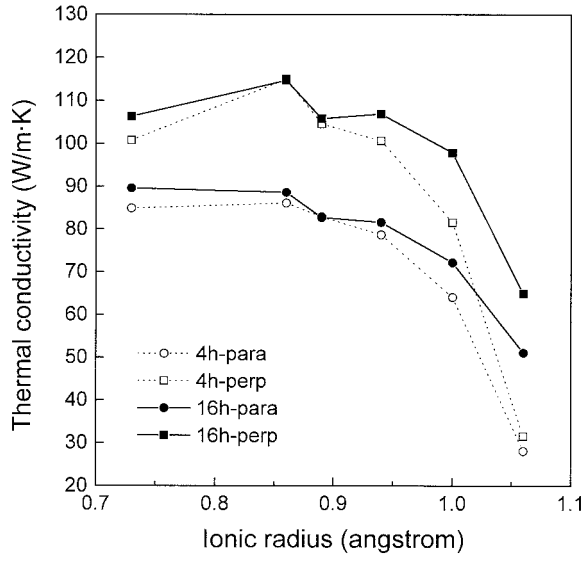

Fig. 4. Relationship between the ionic radii of rare-earth additives and thermal conductivities of the "para" and "perp" specimens of β-Si_3N_4 sintered bodies.

controlled to diffusion-controlled as the ionic radius of the rare-earth element decreases, and later that the activation energy for the interfacial reaction linearly decreases with decreasing ionic radius.[24] This is the reason why the phase transformation rate of a sample sintered with La_2O_3, the largest among the rare-earth ions, is extremely slow, and why mean grain size (≈ mean grain width) increases with decreasing ionic radius of the rare-earth ions.

The reason why the mean grain sizes of samples sintered with Yb_2O_3 and Sc_2O_3 are somewhat smaller than Y_2O_3, even though their grain growth is expected to be more diffusion-controlled, can be attributed to their higher viscosity of the liquid phase due to their higher cationic field strength. Thus, the rare-earth elements with middle ionic radii like Y and Gd give the largest mean grain size. The reason why the mean grain size of a sample sintered with Yb_2O_3 did not increase during 16 h of annealing is unknown. One reason might be the pronounced crystallization of $Yb_4Si_2N_2O_7$, which has a melting point as high as 1870°C,[25] and thus, decreases the amount of the liquid phase at the current annealing temperature of 1850°C. Another reason might be the pronounced vaporization that occurred in a sample sintered with Yb_2O_3. It showed a weight loss as high as about 8% during annealing at 1850°C for 16 h, while the others only showed weight losses of less than 3%. This also might be the reason why the lattice oxygen content of a sample sintered with Yb_2O_3 increased during annealing for 16 h, while all of the others decreased. Since we do not know what kind of species was vaporized, further conclusions are not possible in the present work.

(2) Effect of the Lattice Oxygen Content on Thermal Conductivity

Figure 8 indicates that the lattice oxygen controls the thermal conductivity (diffusivity) of Si_3N_4 ceramics, although Fig. 6 apparently shows the dependency of thermal conductivity (diffusivity) on mean grain size. As of now, we cannot conclude which factor is dominant. However, these two factors are not contradictory, because the larger the ionic radius of the rare-earth element, the finer the mean grain size, and the larger the lattice oxygen content becomes, both of which decrease the thermal conductivity (diffusivity) of β-Si_3N_4 sintered body. The microstructures of β-Si_3N_4 sintered with different rare-earth oxide additives are vastly different, which may not allow us to use the many assumptions that were the basis for analysis via the modified Wiener model.[1] Thus, in this work, we do not make further efforts to eliminate the microstructural effect to extract the effect of the lattice oxygen as was performed in the previous paper.[2]

The reason why the lattice oxygen content decreases with a decrease in the ionic radius of the rare-earth element can be

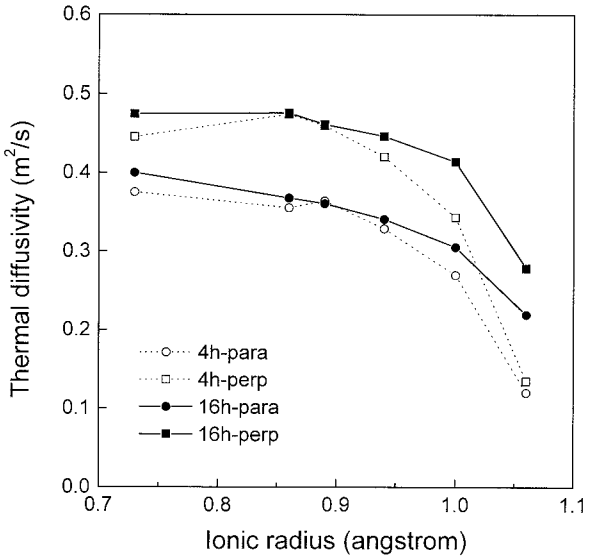

Fig. 5. Relationship between the ionic radii of rare-earth additives and thermal diffusivities of the "para" and "perp" specimens of β-Si_3N_4 sintered bodies.

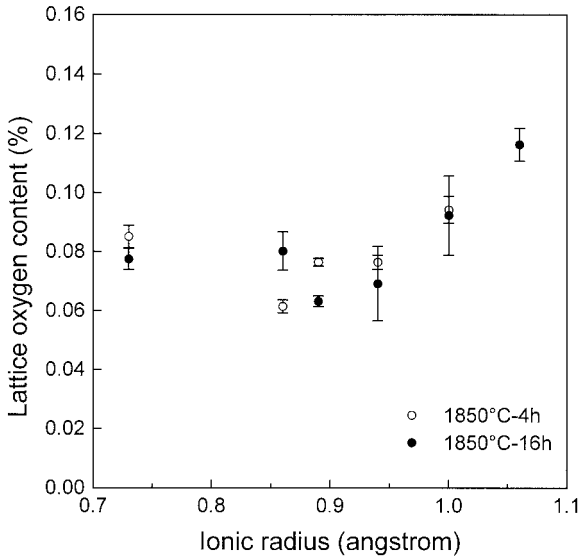

Fig. 7. Relationship between ionic radii of rare-earth oxide additives and lattice oxygen contents of β-Si_3N_4.

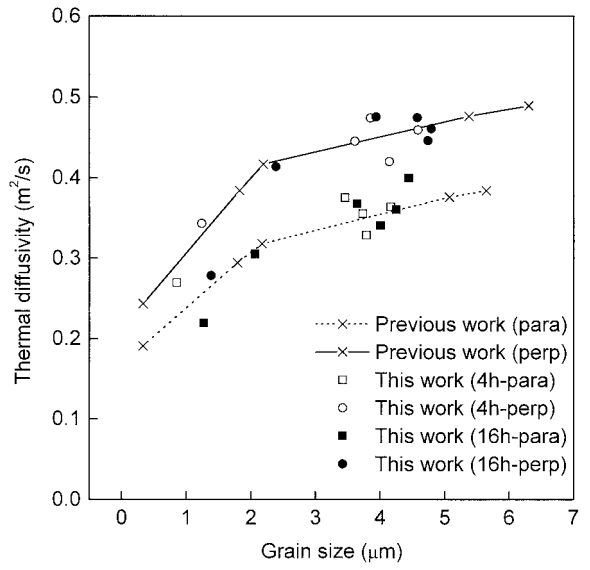

Fig. 6. Comparison of the grain size–thermal diffusivity relationships obtained in this work with the previous data for hot-pressed Si_3N_4 with 5 wt% Y_2O_3.[16]

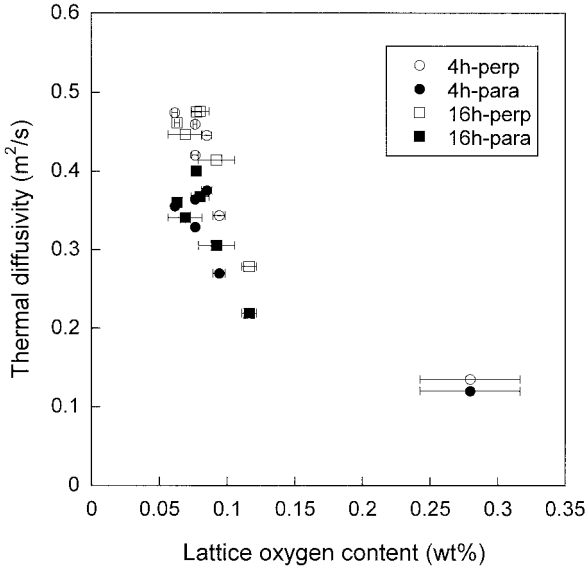

Fig. 8. Relationship between the lattice oxygen content and thermal diffusivity of Si_3N_4 ceramics.

explained simply by the change of the cationic field strength. As the cationic field strength increases with decreasing ionic radius, rare-earth cations attract more oxygen anions, preventing the dissolution of oxygen atoms into the β-Si_3N_4 crystal lattice. The coordination numbers (CNs) of rare-earth ions in the RE-Si-(Al)-O-N liquid phase are not known exactly, and CNs higher than 6 were reported for rare-earth cations.[18] Thus, the application of Pauling's ionic radius (based on a CN of 6) would be too simplistic (and could be wrong). However, there have been a number of works that have shown good correlations between many properties (density, glass transition temperature, thermal expansion coefficient, and so on) of RE-Si-(Al)-O-N glasses and ionic radii of rare-earth ions based on Pauling.[15–18] Ramesh *et al.* found a linear variation in these properties with respect to ionic radius, suggesting that the structures of Ln-Si-Al-O-N glasses are not significantly changed by rare-earth substitution, or in other words, the overall glass structure remains the same and the property changes appear to depend solely on the modifier cationic field strength. A further implication was that the CN was independent of ionic radii, and cationic field strength solely controlled many properties of glasses, because rare-earth cations are the network modifiers that exist out of silicate chains.[18]

In the previous paper (Part II),[2] the phases that appeared after cooling, and hence, thermodynamics, successfully explained the change of the lattice oxygen content. Basically, it was assumed that the liquid phase at the annealing temperature was in equilibrium with the phases observed by XRD. It was suggested that the activity of SiO_2, a_{SiO_2}, in the liquid phase is the lowest when both $Y_{20}N_4Si_{12}O_{48}$ and $Y_2Si_3N_4O_3$ phases coexist as the grain boundary phase of β-Si_3N_4 ceramics sintered with Y_2O_3, which guarantees the highest thermal conductivity for this system. This requires that the Y_2O_3/SiO_2 ratio be more than 10/9. Although the amount of RE_2O_3 was adjusted to make the RE_2O_3/SiO_2 ratio more than 10/9 in this work, the phases appearing were found to be different from those observed for the Y_2O_3 system. The differences in the phases due to different rare-earth oxide additives would partly be the cause for the progressive decrease of the lattice oxygen

contents experimentally observed for RE = La, Nd, and Gd. Higher lattice oxygen contents were observed for samples that contained phases with lower RE_2O_3/SiO_2 ratios, for example, RE_2O_3/SiO_2 = 1/1 and 10/9 for the La_2O_3 system, RE_2O_3/SiO_2 = 2/3 and 1/0 for the Nd_2O_3 system, and RE_2O_3/SiO_2 = 10/9 and 1/0 for the Gd_2O_3 system.

Since melting points, viscosities, and wetting behaviors differ for different sintering additives, their different effects indeed affect oxygen removal during both the phase transformation and Ostwald ripening that proceed via the solution–reprecipitation through the liquid phase. Thus, it should be noted that the ionic radius (cationic field strength) and grain boundary phases are not the only causes that control the lattice oxygen content. As already pointed out in the Section IV(1), grain growth behavior is vastly different for various rare-earth oxide additives. It is quite plausible that this difference would also influence the kinetics of oxygen removal. Evidently, oxygen removal from the Si_3N_4 crystal lattice took place mostly during the phase transformation process, since the lattice oxygen content decreased from 0.83 to 0.28 to 0.12 wt% according to the phase change from the raw powder (α-Si_3N_4 = 97%), via α–β mixture (α-Si_3N_4 = 44%) to β-Si_3N_4, respectively, for La_2O_3 additive. This indicates the advantage of Si_3N_4 ceramics over AlN ceramics, because there is no such phase transformation for AlN, and oxygen removal from the crystal lattice must take place via Ostwald ripening that is much slower and needs higher temperatures than phase transformation. Further investigation is necessary to seek the most suitable sintering additive(s) that is (are) effective for oxygen removal especially during the phase transformation. This would be the ideal direction since it does not require high temperatures to achieve high thermal conductivity, and maintain the high strength that is characteristic of this material.

V. Conclusion

β-Si_3N_4 ceramics sintered with a series of rare-earth (RE = La, Nd, Gd, Y, Yb and Sc; decreasing order of ionic radius) oxide additives have been fabricated by hot pressing, and their microstructures, lattice oxygen contents, and thermal conductivities have been evaluated. The following conclusions can be drawn based on the current work:

(1) Mean grain size increases, while lattice oxygen content decreases, and hence, thermal conductivity (diffusivity) increases with decreasing ionic radius of the rare-earth element. In all cases, a marked change was observed from La to Nd to Gd, and a little change was observed below them.

(2) Mean grain size showed a good correlation with thermal conductivity (diffusivity), and fitted well with the previous relationship. Lattice oxygen content showed a good inverse correlation with thermal conductivity (diffusivity).

(3) As of now, we cannot conclude which factor, microstructure or lattice oxygen content, is dominant. However, these two factors are not contradictory, and there might be a close connection between grain growth kinetics and oxygen removal. The most important conclusion is that rare-earth oxide additives significantly change the thermal conductivity of β-Si_3N_4 ceramics unlike in the case of AlN ceramics. Further investigation is necessary to seek the most suitable sintering additive(s) that is (are) effective for oxygen removal, especially during phase transformation.

References

[1]M. Kitayama, K. Hirao, M. Toriyama, and S. Kanzaki, "Thermal Conductivity of β-Si_3N_4: I, Effects of Various Microstructural Factors," *J. Am. Ceram. Soc.*, **82** [11] 3105–12 (1999).

[2]M. Kitayama, K. Hirao, A. Tsuge, K. Watari, M. Toriyama, and S. Kanzaki, "Thermal Conductivity of β-Si_3N_4: II, Effect of Lattice Oxygen," *J. Am. Ceram. Soc.*, **83** [8] 1985–92 (2000).

[3]K. S. Mazdiyasni and C. M. Cooke, "Consolidation, Microstructure, and Mechanical Properties of Si_3N_4 Doped with Rare-Earth Oxides," *J. Am. Ceram. Soc.*, **57** [12] 536–37 (1974).

[4]P. E. D. Morgan, F. F. Lange, D. R. Clarke, and B. I. Davis, "A New Si_3N_4 Material: Phase Relations in the System Si-Sc-O-N and Preliminary Property Studies," *J. Am. Ceram. Soc.*, **60** [4] C-77–C-78 (1981).

[5]W. A. Sanders and D. M. Mieskowski, "Strength and Microstructure of Sintered Si_3N_4 wih Rare-Earth Oxide Additions," *Am. Ceram. Soc., Bull.*, **64** [2] 304–309 (1985).

[6]E. Tani, S. Umebayashi, K. Kishi, K. Kobayashi, and M. Nishijima, "Gas-Pressure Sintering of Si_3N_4 with Concurrent Addition of Al_2O_3 and 5 wt% Rare Earth Oxide: High Fracture Toughness Si_3N_4 with Fiber-like Structure," *Am. Ceram. Soc. Bull.*, **65** [9] 1311–15 (1986).

[7]N. Hirosaki, A. Okada, and K. Matoba, "Sintering of Si_3N_4 with the Addition of Rare-Earth Oxides," *J. Am. Ceram. Soc.*, **71** [3] C-144–C-147 (1988).

[8]N. Hirosaki, A. Okada, and Y. Akimune, "Gas-Pressure Sintering of Silicon Nitride Containing Small Amounts of Oxide Additives," *J. Mater. Sci. Lett.*, **9,** 1322–23 (1990).

[9]N. Hirosaki, Y. Okamoto, M. Ando, F. Munakata, and Y. Akimune, "Thermal Conductivity of Gas-Pressure-Sintered Silicon Nitride," *J. Am. Ceram. Soc.*, **79** [11] 2878–82 (1996).

[10]H. Park, H.-E. Kim, and K. Niihara, "Microstructural Evolution and Mechanical Properties of Si_3N_4 with Yb_2O_3 as a Sintering Additive," *J. Am. Ceram. Soc.*, **80** [3] 750–56 (1997).

[11]Z.-K. Huang, A. Rosenflanz, and I-W. Chen, "Pressureless Sintering of Si_3N_4 Ceramic Using AlN and Rare-Earth Oxides," *J. Am. Ceram. Soc.*, **80** [5] 1256–62 (1997).

[12]W.-H. Lee, H.-E. Kim, and S.-J. Cho, "Microstructural Evolution of Gas-Pressure-Sintered Si_3N_4 with Yb_2O_3 as a Sintering Aid," *J. Am. Ceram. Soc.*, **80** [10] 2737–40 (1997).

[13]K. Negita, "Ionic Radii and Electronegativities of Effective Sintering Aids for Si_3N_4 Ceramics," *J. Mater. Sci. Lett.*, **4,** 417–18 (1985).

[14]K. Negita, "Effective Sintering Aids for Si_3N_4 Ceramics," *J. Mater. Sci. Lett.*, **4,** 755–58 (1985).

[15]M. Ohashi, K. Nakamura, K. Hirao, S. Kanzaki, and S. Hampshire, "Formation and Properties of Ln-Si-O-N Glasses (Ln = Lanthanides or Y)," *J. Am. Ceram. Soc.*, **78** [1] 71–76 (1995).

[16]J. E. Shelby and J. T. Kohli, "Rare-Earth Aluminosilicate Glasses," *J. Am. Ceram. Soc.*, **73** [1] 39–42 (1990).

[17]S. Tanabe, K. Hirao, and N. Soga, "Elastic Properties and Molar Volume of Rare-Earth Aluminosilicate Glasses," *J. Am. Ceram. Soc.*, **75** [3] 503–506 (1992).

[18]R. Ramesh, E. Nestor, M. J. Pomery, and S. Hampshire, "Formation of Ln-Si-Al-O-N Glasses and Their Properties," *J. Eur. Ceram. Soc.*, **17,** 1933–39 (1997).

[19]M. J. Hoffmann, "Analysis of Microstructural Development and Mechanical Properties of Si_3N_4 Ceramics"; pp. 59–72 in *Tailoring of Mechanical Properties of Si_3N_4 Ceramics*. Edited by M. J. Hoffmann and G. Petzow. Kluwer Academic Publishers, Dordrecht, Netherlands, 1994.

[20]M. Kitayama, K. Hirao, M. Toriyama, and S. Kanzaki, "Control of β-Si_3N_4 Crystal Morphology and Its Mechanism: II, Effect of Lanthanide Additives," *J. Ceram. Soc. Jpn.*, **107** [11] 995–1000 (1999).

[21]T. B. Jackson, A. V. Virkar, K. L. More, R. B. Dinwiddie Jr., and R. A. Cutler, "High-Thermal-Conductivity Aluminum Nitride Ceramics: The Effect of Thermodynamic, Kinetic, and Microstructural Factors," *J. Am. Ceram. Soc.*, **80** [6] 1421–35 (1997).

[22]K. Watari, Y. Seki, and K. Ishizaki, "Temperature Dependence of Thermal Coefficients for HIPped Silicon Nitride," *J. Ceram. Soc. Jpn.*, **97** [2] 174–81 (1989).

[23]*Phase Diagrams for Ceramics*. Compiled at the National Institute of Standards and Technology. Edited and published by the American Ceramic Society.

[24]M. Kitayama, K. Hirao, M. Toriyama, and S. Kanzaki, unpublished work.

[25]T. Nishimura and M. Mitomo, "Phase Relationships in the System Si_3N_4–SiO_2–Yb_2O_3," *J. Mater. Res.*, **10,** 240–42 (1995). □